Ruthenium(II) Complexes Bearing Carboxylato and 2-Oxocarboxylato Ligands

Rainer Müller,[a] Eike Hübner,[a] and Nicolai Burzlaff*[a]

Keywords: Scorpionate ligands / Ruthenium / Bioinorganic chemistry / Tripodal ligands

The syntheses of ruthenium(II) acetato and benzoato complexes [Ru(bdmpza)(O_2CCH_3)(PPh_3)] (**6**) and [Ru(bdmpza)(O_2CPh)(PPh_3)] (**7**) [bdmpza = bis(3,5-dimethylpyrazol-1-yl)-acetate] are reported. The complexes **6** and **7** are synthesized in high yield from [Ru(bdmpza)Cl(PPh_3)$_2$] (**1**) and thallium acetate (**2**) or thallium benzoate (**3**). In a similar substitution reaction a benzoylformate complex [Ru(bdmpza){$O_2CC(O)Ph$}(PPh_3)] (**8**) is obtained from **1** and thallium benzoylformate (**4**). Reaction of **6** or **7** with benzoylformic acid also yields **8**. In analogous reactions several 2-oxocarboxylato ruthenium(II) complexes [Ru(bdmpza){$O_2CC(O)R$}(PPh_3)] (**9**: R = $CH_2CH_2CO_2H$, **10**: R = Me, **11**: R = Et) can be obtained. The low-spin ruthenium(II) complexes **8** to **11** exhibit a purple or brownish-red colour caused by MLCT transitions and thus a HOMO–LUMO gap which is almost identical to that of high-spin 2-oxoglutarate dependent iron oxygenases. **6** crystallises as a water adduct, **6**·H_2O and **8** forms an acetonitrile adduct **12**. Crystal structures of the water adduct **6**·H_2O and **8** were obtained.

Introduction

In recent years the 2-His-1-carboxylate facial triad, an iron binding motif that is found in the active sites of mononuclear non-heme iron(II) and iron(III) dependent enzymes, has attracted increasing interest.[1] The class of 2-oxoglutarate (α-ketoglutarate) dependent iron(II) enzymes, especially, are representative examples of such enzymes. Two iron binding histidines and one aspartate are conserved throughout many of these enzymes.[2] Several protein structures of 2-oxoglutarate (2-OG) dependent iron(II) enzymes have been solved in the last decade, such as deacetoxycephalosporin C synthase (DAOCS),[3] clavaminic acid synthase (CAS),[4] proline hydroxylase,[5] taurine dioxygenase (TauD) (Figure 1)[6] or anthocyanidin synthase (ANS).[7]

Pseudo-kinetic X-ray diffraction experiments on the related enzyme isopenicillin N synthase (IPNS)[2] showed several changes in the electron density close to the substrate but no changes to the 2-His-1-carboxylate facial triad throughout the catalytic cycle.[8] This fixed geometry of the three iron binding amino acids renders them perfect targets for structural model complexes. Especially bulky hydridotris-(pyrazol-1-yl)borato (Tp) and tris(2-pyridylmethyl)amine (TPA) have been used to mimic the active sites of these enzymes.[9,10] Iron benzoylformate complexes with Tp, TPA or TPA-related ligands have been investigated as structural models for more than ten years.[11,12] Recently, we reported on the bis(3,5-dimethylpyrazol-1-yl)acetato ligand

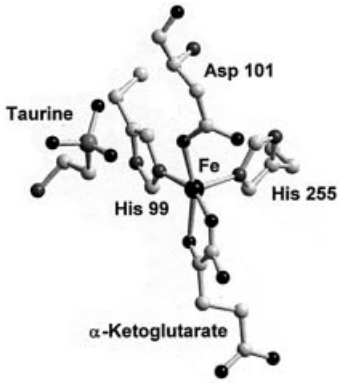

Figure 1. Active site of taurine dioxygenase TauD with 2-oxoglutarate bound to iron(II) and taurine substrate (PDB-Code: 1GY9)[6]

(bdmpza) and its application in ferrous and ferric iron complexes [Fe(bdmpza)$_2$] and [NEt_4][Fe(bdmpza)Cl_3].[13,14] The mono-anionic heteroscorpionate ligand proved, in these cases, to be a promising structural mimic for the facial 2-His-1-carboxylate triad. The O_2 adduct formation and oxygen-activation, key steps in the catalytic pathway of 2-oxoglutarate dependent enzymes, have also been studied upon oxygen-treatment of ruthenium(II) complexes with Tp or trispyridylalkoxymethane ligands.[15] Ruthenium(II) bis(pyrazol-1-yl)acetato complexes such as [Ru(bdmpza)Cl(PPh_3)$_2$] or enantiopure [Ru(bpa^{4cam})Cl(PPh_3)$_2$] and [Ru(bpa^{4menth})-Cl(PPh_3)$_2$] {bpa^{4cam}: bis[4,5,6,7-tetrahydro-7,8,8-trimethyl-(4*S*,7*R*)-methano-N^1,N^1-indazolyl]acetate; bpa^{4menth}: bis[4,5,6,7-tetrahydro-(4*R*)-methyl-(7*R*)-isopropyl-N^1,N^1-indazolyl]-acetate} have recently been described by us.[16,17] We now report on ruthenium(II) bis(3,5-dimethylpyrazol-1-yl)acet-

[a] Fachbereich Chemie der Universität Konstanz,
Universitätsstraße 10, Fach M728,
78457 Konstanz, Germany
Fax: (internat.) + 49-(0)7531-88-3136
E-mail: nicolai@chemie.uni-konstanz.de

ato complexes bearing carboxylato or 2-oxocarboxylato ligands.

Results and Discussion

Ferrous iron complexes with N,N,O ligands are often difficult to investigate, due to their paramagnetic high-spin constitution, and they are very sensitive to oxidation and ligand exchange. In contrast, ruthenium(II) complexes are low spin and thus suitable for NMR characterisation and are also easier to handle. In our attempt to find suitable models for the active site of 2-oxoglutarate dependent iron enzymes, we therefore focused on bis(3,5-dimethylpyrazol-1-yl)acetato ruthenium(II) complexes.

The complex [Ru(bdmpza)Cl(PPh_3)$_2$] (**1**) reacts slowly with thallium carboxylates Tl[O_2CR] (**2**: R = Me, **3**: R = Ph) to produce the $\kappa^2O^1,O^{1\prime}$-carboxylato complexes [Ru(bdmpza)(O_2CR)(PPh_3)] **6** and **7** through loss of one PPh_3 and the chloro ligand (Scheme 1).

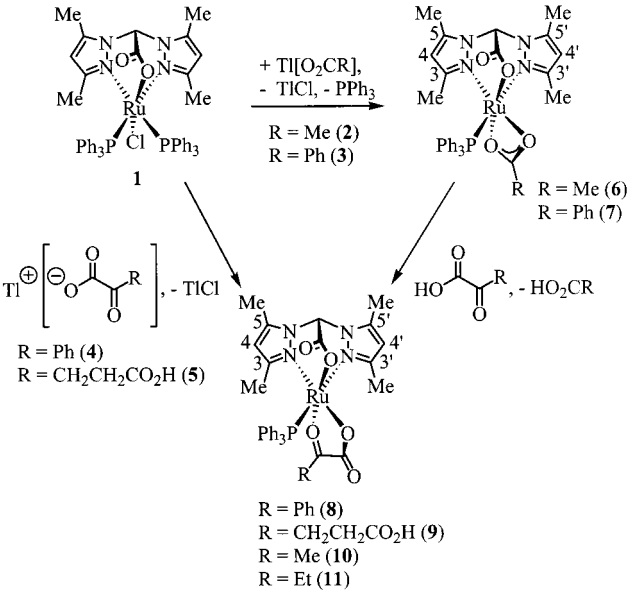

Scheme 1. Formation of carboxylato and 2-oxocarboxylato ruthenium(II) complexes

The thallium benzoate (**3**) and thallium 2-oxocarboxylates (see below) used in this work are easily available by the reaction of thallium acetate with benzoic acid or 2-oxocarboxylic acids [Equation (1)].

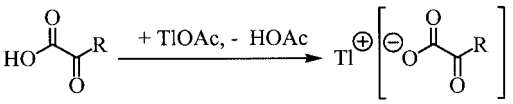

R = Ph (**4**)
R = $CH_2CH_2CO_2H$ (**5**) (1)

These syntheses take advantage of the lower pK_a values of these acids (benzoic acid: 4.22, benzoylformic acid: 1.2, 2-oxoglutaric acid: 2.31/5.14, pyruvic acid: 2.49) compared with acetic acid (4.76).[18] The free acetic acid is distilled off with water as an azeotrope and the thallium carboxylates are obtained in high purity.

Two sets of ^{1}H and ^{13}C signals are detected for the pyrazolyl groups of the bdmpza ligand. Therefore a chiral geometry with a PPh_3 *trans* to one of the pyrazolyl groups has to be assumed for **6** and **7**. A single ^{31}P NMR signal for each of the resulting ruthenium(II) complexes at δ = 62.0 ppm (**6**) and 60.2 ppm (**7**) proves the loss of one PPh_3. For **6** the ^{1}H NMR signal ($CDCl_3$) at δ = 1.00 ppm and the ^{13}C NMR signals (CD_2Cl_2) at δ = 23.6 ppm and 189.0 ppm are assigned to the acetato ligand. The benzoato ligand of **7** shows ^{13}C NMR signals ($CDCl_3$) at 127.1, 127.5, 131.1, 132.1 and 183.8 ppm. The ^{31}P NMR signals as well as the ^{13}C NMR signals correspond well with those of [Ru(Tp)(η^2-O_2CCHPh_2)(PPh_3)] [^{31}P: 63.7 ppm, ^{13}C(CO_2^-): 186.97 ppm].[19]

Admixing three equivalents of water to an NMR sample of **6** in CD_2Cl_2 causes an additional set of signals besides those of **6** which we assign to the formation of an adduct **6**·H_2O. In particular, a slight high-field shift of the acetate ^{13}C NMR signal (CO_2^-: 187.4 ppm) is indicative of this adduct, **6**·H_2O. The shift is in good agreement with the results recently reported by Alper et al. for the formation of [Ru(OAc)$_2$(H_2O)($Ph_2PProMe$)$_2$].[20] An NMR sample of sodium acetate and three equivalents of water in CD_2Cl_2 shows a ^{13}C NMR signal at δ = 181.6 ppm. Therefore, release of acetate and formation of [Ru(bdmpza)(H_2O)$_2$(PPh_3)][O_2CCH_3] can be excluded. After drying the sample in vacuo, only signals of **6** with no water can be detected. This proves that the formation of **6**·H_2O is fully reversible.

An X-ray structure determination of **6** revealed the water adduct of **6**·H_2O, with H_2O coordinated to ruthenium(II) and a monodentate κ*O*-acetato ligand (Figure 2, Table 1).

An intramolecular hydrogen bond between the water molecule and the non-coordinated oxygen atom of the acetate is indicated by the short distance *d*[O(4)···O(5)] = 2.720(6) Å. The presence of water can be explained by the fact that the crystals were grown under humid conditions and is proven by a CHN analysis of the crystals. Thus, $\kappa^2O^1,O^{1\prime}$-carboxylato ligands are hemilabile, chelating ligands. Once water is present, it can readily displace one of the oxygen atoms of the coordinating carboxylate. A very similar hydrogen bond was recently observed in a DAOCS protein structure presenting a DAOCS:Fe^{II}:CO_2:succinate:H_2O complex.[3b] The ring tension of the metalla-tetracycle is probably reduced by this water coordination.

The reaction of [Ru(bdmpza)Cl(PPh_3)$_2$] (**1**) with thallium 2-oxocarboxylates Tl[O_2CC(O)R] (**4**: R = Ph, **5**: R = $CH_2CH_2CO_2H$) produces κ^2O^1,O^2-2-oxocarboxylato complexes (Scheme 1). Single ^{31}P NMR signals at δ = 57.9 ppm (**8**) and 58.2 ppm (**9**) once again prove the loss of one PPh_3 ligand. Traces of a second structural isomer can be observed at δ = 57.1 ppm for **9**. The coordination of the 2-oxocarboxylates is backed by the [M^+] peaks in the FAB-

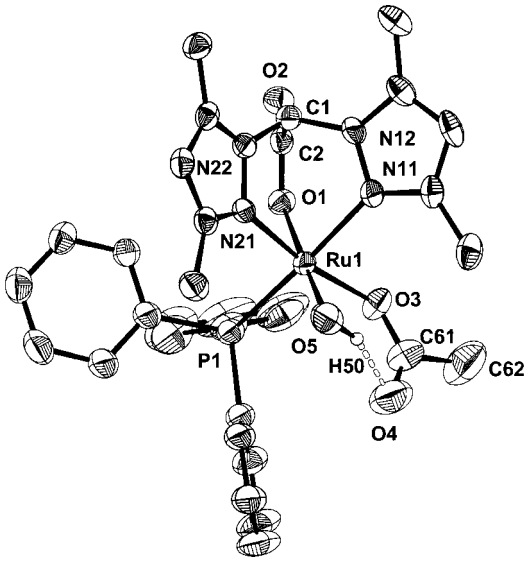

Figure 2. Molecular structure of [Ru(bdmpza)(H_2O)(O_2CCH_3)(PPh_3)] (**6**·H_2O); thermal ellipsoids are drawn at the 50% probability level

Table 1. Selected bond lengths (Å) and angles (°) of complex **6**·H_2O

Ru−N(11)	2.143(3)	C(1)−C(2)	1.547(6)
Ru−N(21)	2.081(4)	C(2)−O(1)	1.295(5)
Ru−O(1)	2.096(3)	C(2)−O(2)	1.231(5)
Ru−O(3)	2.087(3)	C(1)−N(12)	1.469(5)
Ru−O(5)	1.974(3)	C(1)−N(22)	1.446(5)
Ru−P(1)	2.3501(14)	O(3)−C(61)	1.255(6)
O(4)−O(5)	2.720(6)	O(4)−C(61)	1.220(7)
N(11)−Ru−N(21)	83.42(13)	N(11)−Ru−O(3)	86.85(14)
O(1)−Ru−N(11)	86.25(13)	N(11)−Ru−O(5)	91.77(14)
O(1)−Ru−N(21)	87.24(13)	N(21)−Ru−P(1)	98.73(10)
O(1)−Ru−P(1)	85.46(9)	N(21)−Ru−O(3)	170.24(13)
O(1)−Ru−O(3)	91.47(12)	N(21)−Ru−O(5)	91.65(16)
O(1)−Ru−O(5)	177.83(13)	O(3)−Ru−O(5)	89.31(15)
N(11)−Ru−P(1)	171.33(10)	O(3)−C(61)−O(4)	127.1(6)

MS and the ^{13}C NMR signals of the 2-oxo groups (**8**: 202.8 ppm, **9**: 215.5 ppm). Both complexes exhibit one (**8**) and two (**9**) additional CO_2^- signals in the ^{13}C NMR spectra. As to be expected for a chelate binding of the 2-oxocarboxylate, the complexes exhibit a chiral environment and therefore two sets of signals in the ^1H and ^{13}C NMR spectra for the pyrazolyl groups. Due to this chirality in **9**, an ABXY system in the ^1H NMR spectrum can be assigned to CH_2CH_2 of the 2-oxoglutarate. The X-ray structure determination of **8** establishes the chelate binding of the benzoylformate (Figure 3, Table 2).

The most striking feature of this structure is the position of the 2-oxo group *trans* to the carboxylate donor of the bdmpza ligand. This configuration agrees well with the coordination of the 2-oxoglutarate in the active site of 2-oxoglutarate dependent enzymes where the 2-oxo group is found *trans* to the iron binding aspartate (Figure 1).

As shown in Figure 3, the phenyl group of the benzoylformate ligand is almost parallel to one of the phenyl groups of PPh_3. Despite this parallel orientation the torsion

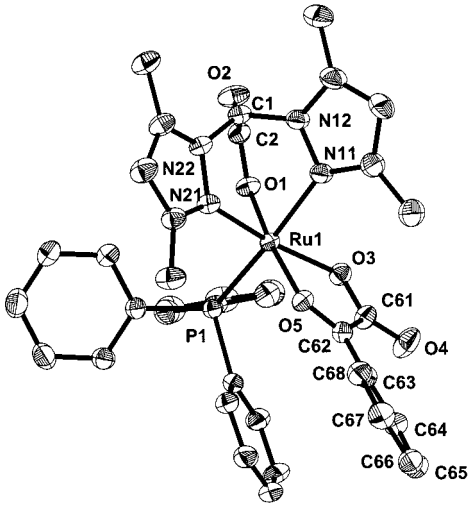

Figure 3. Molecular structure of [Ru(bdmpza){$O_2CC(O)Ph$}(PPh_3)] (**8**); thermal ellipsoids are drawn at the 50% probability level

Table 2. Selected bond lengths (Å) and angles (°) of complex **8**

Ru−N(11)	2.170(3)	C(2)−O(1)	1.292(4)
Ru−N(21)	2.074(3)	C(2)−O(2)	1.224(4)
Ru−O(1)	2.086(3)	C(1)−N(12)	1.466(4)
Ru−O(3)	2.095(2)	C(1)−N(22)	1.451(4)
Ru−O(5)	2.078(3)	O(3)−C(61)	1.282(4)
Ru−P(1)	2.322(2)	O(4)−C(61)	1.237(4)
C(1)−C(2)	1.551(4)	O(5)−C(62)	1.258(4)
N(11)−Ru−N(21)	81.95(11)	N(11)−Ru−O(3)	90.44(11)
O(1)−Ru−N(11)	86.71(11)	N(11)−Ru−O(5)	93.11(11)
O(1)−Ru−N(21)	88.79(11)	N(21)−Ru−P(1)	98.45(9)
O(1)−Ru−P(1)	86.59(9)	N(21)−Ru−O(3)	171.96(9)
O(1)−Ru−O(3)	93.36(11)	N(21)−Ru−O(5)	100.66(11)
O(1)−Ru−O(5)	170.44(8)	O(3)−Ru−O(5)	77.08(10)
N(11)−Ru−P(1)	173.28(7)	O(3)−C(61)−O(4)	125.0(3)

angle O(5)−C(62)−C(63)−C(68) of 20.4° indicates that there is still conjugation to the CO_2^- group via the 2-oxo group. The distances and angles of the [Ru(bdmpza)(PPh_3)] fragments in **6** and **8** agree well with those reported earlier for [Ru(bdmpza)Cl(PPh_3)$_2$] (**1**).[16]

The complexes **8** and **9** can also be obtained in high yield and high purity by reaction of benzoylformic acid and 2-oxoglutaric acid with the acetato complex **6** or the benzoato complex **7**. It is noteworthy, that this exchange of a carboxylato ligand by a 2-oxocarboxylato ligand is similar to the regeneration step of the biocatalytic pathway postulated for the 2-oxoglutarate dependent enzymes. In these enzymes an iron(II) bound succinate is replaced by 2-oxoglutarate to "reload" the active site of the enzyme after the hydroxylation of the substrate.[6]

It is even possible to combine the two synthetic steps: Reaction of the chloro complex **1** with thallium acetate and 2-oxocarboxylic acid affords the 2-oxocarboxylato ruthenium(II) complexes [Ru(bdmpza){$O_2CC(O)R$}(PPh_3)] (**8**: R = Ph, **9**: R = $CH_2CH_2CO_2H$, **10**: R = Me, **11**: R = Et) within 2 h (**8**, **10** and **11**) or 24 h (**9**). The ^{31}P NMR spectra of the complexes **10** and **11** exhibit a single signal

each [δ = 58.1 ppm (**10**) and 58.5 ppm (**11**)]. The coordination of the 2-oxocarboxylates follows from the [M^+] peaks in the FAB MS, the ^{13}C NMR signals assigned to the 2-oxo carbonyl groups (**10**: δ = 215.8 ppm, **11**: δ = 217.9 ppm) and additional CO_2^- signals. Again the complexes are chiral and therefore two sets of signals appear in the ^1H and ^{13}CNMR spectra for the pyrazolyl groups. Complex **11** presents an ABX_3 system in the ^1H NMR spectrum that can be assigned to the CH_2CH_3 group. In some of the IR spectra of **8**−**11** two resonances occur around 1660 cm^{-1} which can be assigned to the two $\nu_{asym}(CO_2^-)$ of the bdmpza ligand and the 2-oxocarboxylate. It was not possible to assign unambiguously $\nu_{sym}(CO_2^-)$ of the complexes **6**−**11** to absorptions in the region of 1300 to 1500 cm^{-1}. This is due to the weakness of the signals and several overlapping absorptions of the PPh_3 ligand in that region.

In the case of **8**, **10** and **11** longer reaction times cause the occurrence of additional NMR signal sets, which are probably due to the formation of structural isomers. A mixture of the isomers was isolated for the 2-oxoglutarate complex **9**. We are currently investigating the character of these minor isomers, which most likely exhibit a geometry that involves the 2-oxo group being *trans* to a pyrazolyl group.

The formation of the 2-oxocarboxylato complexes is clearly indicated by a purple (**8**) or brownish-red (**9**−**11**) colour (Figure 4).

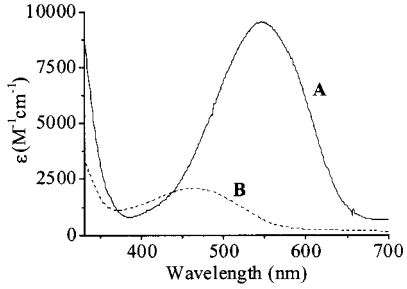

Figure 4. Electronic spectra of (A) [Ru(bdmpza){O_2CC(O)Ph}(PPh_3)] (**8**) (−) and (B) [Ru(bdmpza){O_2CC(O)CH_3}(PPh_3)] (**10**) (--) in CH_2Cl_2. Spectra of **9** and **11** are almost identical to **10**

Also, for the 2-oxoglutarate dependent enzymes, the addition of Fe^{II} and 2-oxoglutarate to the enzymes under anaerobic conditions results in a purple colour with a broad absorption band centred near 530 nm.[10c] The colour has been attributed to charge-transfer transitions from the metal centre to the coordinated 2-oxo group (MLCT absorption).[10c,11d,12c,21] Complexes **8**−**11** exhibit extinction coefficients at 546 nm (**8**) or 463 nm (**9**−**11**), which are almost 20-fold larger than those of the iron(II) models or enzymes {e.g. [Fe^{II}(Tp^{Ph2}){O_2CC(O)Ph}] ε (M^{-1}·cm^{-1}) = 540; [Fe^{II}TauD(2-OG)] ε (M^{-1}·cm^{-1}) = 140}.[10c] To verify this MLCT hypothesis for these ruthenium(II) complexes, extended Hückel[22] and DFT calculations were performed. The calculated HOMO−LUMO energy gaps of the DFT calculations are too small by a factor of about 2.5 compared with the measured, longest $\lambda_{max.}$. This is a well-known behaviour involving the gap between the HOMO−LUMO eigenvalues of DFT calculations, due to theoretical reasons.[23] According to the DFT calculations the band at the longest wavelength should shift to longer wavelengths by about 150 nm when the 2-oxocarboxylato complex **10** (R = Me) is replaced by **8** (R = Ph). Such a shift to longer wavelengths is indeed observed in the UV/Vis spectra, although to a smaller extent (Figure 4). The calculated results could be confirmed by the HOMO−LUMO energy gaps of the Hückel-calculation which also predicts this shift. Contour plots of the HOMO and LUMO for both complexes are shown in Figure 5.

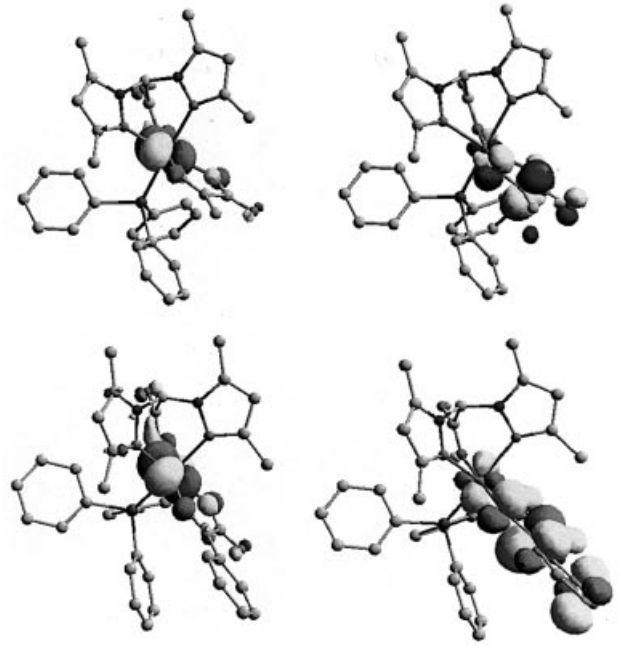

Figure 5. Contour plots of the delocalised HOMO (left) and LUMO (right) (DFT calculation) for **10** (top) and **8** (bottom)

The HOMO is clearly localised at the ruthenium(II) metal centre in **10** as well as in **8**. Two other MOs are only slightly lower in energy in both cases. Contour plots of these three orbitals exhibit geometries that are characteristic for d_{xy}, d_{xz} and d_{yz} orbitals. This is quite reasonable for a $4d^6$ low spin ruthenium(II) complex. Thus, all six d-electrons are available for a HOMO−LUMO transition. As a result of the good orientation of two of the HOMOs towards the LUMO, the HOMO−LUMO orbital overlap in the ruthenium(II) complexes should be better than in the iron complexes or iron enzymes. Moreover, this is true for ruthenium(II) 4d orbitals and not iron(II) 3d orbitals. These findings might explain why the extinction coefficients for the MLCT bands are almost 20-fold larger than those of the iron(II) models or enzymes.

The LUMOs in **8** and **10** are localised at the 2-oxocarboxylato ligands. They are composed of p_z density on the 2-oxo group with some conjugation to the carboxylate p_z. This is in good agreement with the π* LUMO of a coordinated pyruvate which was reported earlier by Solomon.[21] In **8** the LUMO is also delocalised into the aromatic substituent. The missing delocalisation into an aromatic system

can explain the hypsochromic shift of the longest wavelength absorption of **10**. The structure of the LUMO is supported by the results of the Hückel calculations, which deliver a nearly identical electron density distribution.

Therefore, the calculations verify the metal-to-ligand charge transfer (MLCT). Although the ruthenium(II) complexes **8** and **10** have a low-spin t_{2g}^6 configuration they exhibit a HOMO−LUMO gap which is almost identical in size to that of the $t_{2g}^4e_g^2$ iron centres of the enzymes.

A solution of the benzoylformate complex **8** in acetonitrile changes its colour from purple to yellow upon heating. This can be explained by the formation of an adduct [Ru(bdmpza){$O_2CC(O)Ph$}($NCCH_3$)(PPh_3)] (**12**) with the solvent acetonitrile. A similar behaviour was reported earlier for 2-oxocarboxylato iron complexes.[11b,12] Besides the colour change the adduct formation is documented by IR and ^1H NMR spectroscopic data as well as an 802 [MH^+] peak in the FAB-MS. Due to the rather labile coordination of CH_3CN in **12** we were unable to obtain a correct CHN elemental analysis and ^{13}C NMR spectroscopic data.

Therefore, the 2-oxocarboxylates as well as the carboxylates are hemilabile ligands and should render the additional coordination of reactive species possible. Although **8** seems to be rather stable under aerobic conditions, a solution of **8** in 1,2-dichloroethane, when exposed to air, decomposed within two weeks to form red crystals of the ruthenium(III) complex [Ru(bdmpza)Cl_2(PPh_3)] (**13**), which we reported recently.[16] Further work will focus on these oxidation reactions.

Experimental Section

General Remarks: All operations were carried out under either nitrogen or argon by using conventional Schlenk techniques. Solvents were distilled from appropriate drying agents and degassed before use. The yields refer to analytically pure compounds and were not optimised. IR: Biorad FTS 60, CaF_2 cuvettes (0.5 mm). ^1H NMR and ^{13}C NMR: Bruker AC 250, Varian Inova-400, δ values relative to TMS. ^{31}P NMR: JEOL GX 400, Bruker DRX 600 Avance, δ values relative to an external standard from Wilmad (H_3PO_4 100%). 2D NMR experiments: Bruker DRX 600 Avance, Varian Inova-400. Mass spectra were recorded on a modified Finnigan MAT 312 using the FAB technique and 3-nitrobenzyl alcohol as matrix. Elemental analyses: Heraeus CHN−O-Rapid. UV/Vis: Hewlett−Packard Diode-Array spectrophotometer 8452A (silica cuvette; d = 1 cm). A modified Siemens P4 diffractometer was used for X-ray structure determination.

Thallium acetate (**2**), benzoic acid, pyruvic acid, 2-oxobutyric acid, benzoylformic acid and 2-oxoglutaric acid were used as purchased. Ruthenium(III) trichloride hydrate was a generous gift of the Degussa AG. The synthesis of [Ru(bdmpza)Cl(PPh_3)$_2$] (**1**) was reported recently.[16]

Method A. General Procedure for the Synthesis of Thallium Carboxylates: Equimolar amounts of thallium acetate (**2**) and the carboxylic acid were dissolved in water. The water/HOAc mixture was removed by azeotropic distillation and the procedure was repeated once. The remaining residue was washed with acetone and re-crystallised from acetone/water to yield thallium carboxylate suitable for further reactions.

Method B. General Procedure for the Synthesis of Carboxylato Ruthenium(II) Complexes: A solution of [Ru(bdmpza)Cl(PPh_3)$_2$] (**1**) and a slight excess of thallium carboxylate in CH_2Cl_2 was stirred at ambient temperature. The mixture was filtered through celite and dried in vacuo. Precipitation from CH_2Cl_2 solution with pentane yielded the carboxylato ruthenium(II) complex.

Method C. General Procedure for the Synthesis of Ruthenium(II) 2-Oxocarboxylato Complexes: A solution of [Ru(bdmpza)Cl(PPh_3)$_2$] (**1**), a slight excess of thallium acetate and an excess of a 2-oxocarboxylic acid were stirred in CH_2Cl_2 at ambient temperature. The mixture was filtered through celite and dried in vacuo. Precipitation from CH_2Cl_2 solution with pentane yielded the 2-oxocarboxylato ruthenium(II) complex.

Tl[O_2CPh] (3): Reaction of thallium acetate (**2**) (2.01 g, 7.63 mmol) and benzoic acid (0.933 g, 7.64 mmol) in water (2 × 100 mL) according to procedure A yielded **3** as a white microcrystalline powder. Yield 1.99 g (80%); m.p. > 300 °C. ^1H NMR (D_2O + 1% v/v [D_6]acetone, 250 MHz): δ = 7.30−7.41 (m, 3 H, *p*-Ph and *m*-Ph), 7.73 (m, 2 H, *o*-Ph) ppm. ^{13}C NMR (D_2O + 1% v/v [D_6]acetone, 62.9 MHz): δ = 129.7, 130.2, 132.7, 137.6 (Ph), 176.8 (CO_2^-) ppm. $C_7H_5O_2Tl$ (325.50): calcd. C 25.83, H 1.55; found C 26.00, H 1.68.

Tl[$O_2CC(O)Ph$] (4): Reaction of thallium acetate (**2**) (2.01 g, 7.63 mmol) and benzoylformic acid (1.22 g, 8.13 mmol) in water (2 × 50 mL) according to procedure A yielded **4** as a white microcrystalline powder. Yield 2.50 g (93%); m.p. 140 °C (dec.). ^1H NMR (D_2O +1% v/v [D_6]acetone, 250 MHz): δ = 7.45 (vt, 2 H, *m*-Ph), 7.61 (t, 1 H, *p*-Ph), 7.81 (d, 2 H, *o*-Ph) ppm. ^{13}C NMR (D_2O +1% v/v [D_6]acetone, 62.9 MHz): δ = 129.5, 130.0, 132.3, 135.5 (Ph), 173.0 (CO_2^-), 197.0 (CO) ppm. $C_8H_5O_3Tl$ (353.51): calcd. C 27.18, H 1.43; found C 27.36, H 1.31.

Tl[$O_2CC(O)CH_2CH_2CO_2H$] (5): Reaction of thallium acetate (**2**) (1.00 g, 3.80 mmol) and 2-oxoglutaric acid (555 mg, 3.80 mmol) in water (50 mL) according to procedure A yielded crude **5** after removing HOAc and H_2O at 55 °C and reduced pressure. Re-crystallisation from H_2O/Acetone yielded white microcrystalline powder. Yield 1.20 g (90%); m.p. 130 °C (dec.). ^1H NMR (D_2O + 1% v/v [D_6]acetone, 250 MHz): δ = 2.49 (t, $^3J_{H,H}$ = 6.6 Hz, 2 H, $CH_2CO_2^-$), 2.85 (t, $^3J_{H,H}$ = 6.6 Hz, 2 H, CH_2CO) ppm. ^{13}C NMR (D_2O + 1% v/v [D_6]acetone, 62.9 MHz): δ = 28.6 (CH_2CO), 34.6 ($CH_2CO_2^-$), 170.3 (CO_2^-), 178.6 (CO_2H) ppm. $C_5H_5O_5Tl$ (349.47): calcd. C 17.18, H 1.44; found C 16.82, H 1.40.

[Ru(bdmpza)(O_2CCH_3)(PPh_3)] (6): Reaction of [Ru(bdmpza)-Cl(PPh_3)$_2$] (**1**) (663 mg, 0.730 mmol) and thallium acetate **2** (235 mg, 0.892 mmol) in CH_2Cl_2 (50 mL) according to method B yielded product **6** as a yellow solid after 60 h. Yield 0.367 g (75%); m.p. 200 °C (dec.). ^1H NMR ($CDCl_3$, 250 MHz): δ = 1.00 (s, 3 H, Ac−CH_3), 1.77 (s, 3 H, C^3−CH_3), 2.41 (s, 3 H, $C^{3'}$−CH_3), 2.44 (s, 3 H, C^5−CH_3), 2.51 (s, 3 H, $C^{5'}$−CH_3), 5.68 (s, 1 H, H_{pz}), 6.11 (s, 1 H, $H_{pz'}$), 6.36 (s, 1 H, CH), 7.15−7.75 (m, 15 H, PPh_3) ppm. ^1H NMR (CD_2Cl_2, 400 MHz): δ = 0.93 (s, 3 H, Ac−CH_3), 1.66 (s, 3 H, C^3−CH_3), 2.31 (s, 3 H, $C^{3'}$−CH_3), 2.35 (s, 3 H, C^5−CH_3), 2.42 (s, 3 H, $C^{5'}$−CH_3), 5.62 (s, 1 H, H_{pz}), 6.06 (s, 1 H, $H_{pz'}$), 6.23 (s, 1 H, CH), 7.05−7.40 (m, 15 H, PPh_3) ppm. ^{13}C NMR ($CDCl_3$, 62.9 MHz): δ = 11.2 (C^5−CH_3), 11.5 ($C^{5'}$−CH_3), 12.5 ($C^{3'}$−CH_3), 14.6 (C^3−CH_3), 23.5 (Ac−CH_3), 68.8 (CH), 108.0 (C^4), 109.2 ($C^{4'}$), 127.8 (d, $^3J_{C,P}$ = 9.1 Hz, *m*-PPh_3), 129.1 (*p*-PPh_3), 134.3 (br., *o*-PPh_3), 140.9 ($C^{5'}$), 142.2 (C^5), 155.0 (C^3), 158.2 ($C^{3'}$), 168.2 (CO_2^-), 188.7 (CO_2^-) ppm. ^{13}C NMR (CD_2Cl_2, 100.5 MHz): δ = 11.2 (C^5−CH_3), 11.5 ($C^{5'}$−CH_3), 12.5 ($C^{3'}$−CH_3), 14.5 (C^3−CH_3), 23.6 (Ac−CH_3), 69.0 (CH), 108.2 (C^4), 109.3 (d, $^4J_{C,P}$ = 2.8 Hz, $C^{4'}$), 128.0 (d, $^3J_{C,P}$ = 9.2 Hz, *m*-PPh_3), 129.4 (*p*-PPh_3), 134.3 (br., *o*-

PPh_3), 141.6 ($C^{5'}$), 143.1 (C^5), 155.2 (d, $^3J_{C,P}$ = 2.7 Hz, C^3), 158.3 ($C^{3'}$), 168.1 (CO_2^-), 189.0 (CO_2^-) ppm. ^{31}P NMR ($CDCl_3$, 161.8 MHz): δ = 62.0 ppm. IR (THF): $\tilde{\nu}$ = 1674 vs (CO_2^-), 1653 w, 1560 w (C=N), 1464 m, 1436 m, 1420 w cm^{-1}. IR (CH_2Cl_2): $\tilde{\nu}$ = 1661 vs (CO_2^-), 1563 w (C=N), 1483 w, 1463 m, 1435 m, 1418 w cm^{-1}. IR (KBr): $\tilde{\nu}$ = 1668 vs (CO_2^-), 1585 w, 1563 m (C=N), 1482 w, 1462 m, 1434 m, 1418 w cm^{-1}. UV/Vis (CH_2Cl_2): $\lambda_{max.}$ (log ε) = 233.0 (4.37) nm. EI-MS (70 eV, 370 °C): *m*/*z* (%) = 670 (3) [M^+], 626, (1) [$M^+ - CO_2$], 566 (3) [$M^+ - CO_2 - HOAc$]. FAB-MS (NBOH): *m*/*z* (%) = 748 (83) [$M^+ + H_2O + HOAc$], 670 (100) [M^+], 611 (39) [$M^+ - OAc$], 566 (44) [$M^+ - CO_2 - HOAc$]. $C_{32}H_{33}N_4O_4PRu$ (669.68): calcd. C 57.39, H 4.97, N 8.37; found C 56.88, H 5.34, N 8.36.

Reaction of 6 with H_2O. Formation of [Ru(bdmpza)(OAc)(H_2O)(PPh_3)] (6·H_2O): Three equivalents of water (6.00 μL, 0.336 mmol) were added to an NMR sample of [Ru(bdmpza)(OAc)(PPh_3)] (**6**) (75 mg, 0.112 mmol) in CD_2Cl_2 (0.7 mL). NMR spectra were immediately recorded, showing new signals besides those of **6**, due to the presence of **6**·H_2O. ^1H NMR (CD_2Cl_2, 400 MHz): δ = 1.50, 1.65, 2.06, 2.25, 2.45 (s, some signals are broad and covered, 5 × CH_3 and H_2O), 5.80 (s, 1 H, H_{pz} or $H_{pz'}$), 5.89 (s, 1 H, H_{pz} or $H_{pz'}$), 6.41 (s, 1 H, CH), 7.05−7.40 (m, 15 H, PPh_3) ppm. ^{13}C NMR (CD_2Cl_2, 100.5 MHz): δ = 10.9, 12.9, 13.0, 14.0 (4 × CH_3), 24.8 (Ac−CH_3), 69.5 (CH), 108.8, 109.2 (C^4 and $C^{4'}$), PPh_3 signals covered, 141.8, 143.7 (C^5 and $C^{5'}$), 154.5, 159.1 (C^3 and $C^{3'}$), 168.7 (CO_2^-), 187.4 (CO_2^-) ppm. ^{31}P NMR (CD_2Cl_2, 161.8 MHz): δ = 57.1 ppm. Crystallisation of **6** with CH_2Cl_2/hexane under humid conditions yielded yellow crystals of the adduct **6**·H_2O. M.p. 200−205 °C (dec.). FAB-MS (NBOH): *m*/*z* (%) = 748 (18) [$M^+ + H_2O + HOAc$], 670 (100) [M^+], 611 (31) [$M^+ - OAc$], 566 (37) [$M^+ - CO_2 - HOAc$]. Crystals: $C_{32}H_{33}N_4O_4PRu{\cdot}CH_2Cl_2{\cdot}H_2O$ (772.63): calcd. C 51.30, H 4.83, N 7.25; found C 51.56, H 4.54, N 7.30.

[Ru(bdmpza)(O_2CPh)(PPh_3)] (7): Reaction of [Ru(bdmpza)Cl(PPh_3)$_2$] (**1**) (493 mg, 0.543 mmol) with thallium benzoate (**3**) (212 mg, 0.651 mmol) in CH_2Cl_2 (40 mL) according to method B yielded product **7** as a pale yellow microcrystalline powder after 60 h. Yield 298 mg (75%); m.p. 130 °C (dec.). ^1H NMR ($CDCl_3$, 600 MHz): δ = 1.87 (s, 3 H, C^3-CH_3), 2.22 (s, 3 H, $C^{3'}-CH_3$), 2.45 (s, 3 H, C^5-CH_3), 2.50 (s, 3 H, $C^{5'}-CH_3$), 5.71 (s, 1 H, H_{pz}), 6.05 (s, 1 H, $H_{pz'}$), 6.38 (s, 1 H, CH), 7.13−7.51 (m, 20 H, Ph & PPh_3) ppm. ^{13}C NMR ($CDCl_3$, 150.9 MHz): δ = 11.2 (C^5-CH_3), 11.5 ($C^{5'}-CH_3$), 13.0 ($C^{3'}-CH_3$), 14.8 (C^3-CH_3), 68.9 (CH), 108.1 (C^4), 109.2 ($C^{4'}$), 127.1 (*m*-Ph), 127.5 (*o*-Ph), 127.7 (d, $^3J_{C,P}$ = 9.2 Hz, *m*-PPh_3), 129.0 (*p*-PPh_3), 131.1 (*p*-Ph), 132.1 (*i*-Ph), 134.2 (br., *o*-PPh_3), 140.8 (C^5), 142.2 ($C^{5'}$), 155.3 ($C^{3'}$), 158.3 (C^3), 168.2 (CO_2^-), 183.8 (CO_2^-) ppm. ^{31}P NMR ($CDCl_3$, 161.8 MHz): δ = 60.2 ppm. IR (CH_2Cl_2): $\tilde{\nu}$ = 1662 vs (CO_2^-), 1645 w, 1563 w (C=N), 1505 w, 1501 w, 1482 w, 1463 w, 1435 m, 1428 m, 1419 w cm^{-1}. IR (KBr): $\tilde{\nu}$ = 1671 vs (CO_2^-), 1561 w (C=N), 1499 w, 1482 w, 1460 w, 1431 m, 1421 sh cm^{-1}. UV/Vis (CH_2Cl_2): $\lambda_{max.}$ (log ε) = 235.0 (4.43), 316.0 (3.91) nm. FAB-MS (NBOH): *m*/*z* (%) = 732 (100) [M^+], 611 (41) [$M^+ - O_2CPh$], 566 (38) [$M^+ - CO_2 - HO_2CPh$]. $C_{37}H_{35}N_4O_4PRu{\cdot}H_2O$ (749.77): calcd. C 59.27, H 4.97, N 7.47; found C 59.30, H 5.30, N 7.46.

[Ru(bdmpza){$O_2CC(O)Ph$}(PPh_3)] (8): Reaction of [Ru(bdmpza)Cl(PPh_3)$_2$] (**1**) (333 mg, 0.367 mmol), thallium acetate (**2**) (115 mg, 0.437 mmol) and benzoylformic acid (69.0 mg, 0.460 mmol) in CH_2Cl_2 (30 mL) according to method C yielded product **8** as a dark purple microcrystalline powder after 2 h. Yield 253 mg (91%); m.p. 240 °C (dec.). ^1H NMR ($CDCl_3$, 600 MHz): δ = 1.88 (s, 3 H, $C^{3'}-CH_3$), 1.89 (s, 3 H, C^3-CH_3), 2.47 (s, 3 H, C^5-CH_3), 2.49 (s, 3 H, $C^{5'}-CH_3$), 5.80 (s, 1 H, $H_{pz'}$), 5.93 (s, 1 H, H_{pz}), 6.45 (s, 1 H, CH), 7.20 (m, 6 H, *m*-PPh_3), 7.26 (m, 3 H, *p*-PPh_3), 7.32 (m, 6 H, *o*-PPh_3), 7.33 (m, 2 H, *m*-Ph), 7.52 (t, 1 H, *p*-Ph), 8.33 (d, 2 H, *o*-Ph) ppm. ^{13}C NMR ($CDCl_3$, 150.9 MHz): δ = 11.1 (C^5-CH_3), 11.6 ($C^{5'}-CH_3$), 13.4 (C^3-CH_3), 14.3 ($C^{3'}-CH_3$), 69.0 (CH), 108.8 ($C^{4'}$), 109.2 (C^4), 128.2 (d, $^3J_{C,P}$ = 11.6 Hz, *m*-PPh_3), 128.3 (*m*-Ph), 129.6 (*p*-PPh_3), 130.4 (*o*-Ph), 133.5 (*i*-Ph), 134.1 (d, $^2J_{C,P}$ = 6.9 Hz, *o*-PPh_3), 134.4 (*p*-Ph), 140.9 (C^5), 142.9 ($C^{5'}$), 154.6 (C^3), 158.8 ($C^{3'}$), 168.0 (CO_2^-), 169.7 (CO_2^-), 202.8 (C=O) ppm. ^{31}P NMR ($CDCl_3$, 161.8 MHz): δ = 57.9 ppm. IR (CH_2Cl_2): $\tilde{\nu}$ = 1659 s, 1653 vs (CO_2^-), 1563 (C=N), 1483 w, 1463 w, 1446 w, 1435 w, 1418 w cm^{-1}. IR (KBr): $\tilde{\nu}$ = 1652 br (CO_2^-), 1563 w (C=N), 1482 w, 1461 w, 1446 w, 1434 w, 1418 w cm^{-1}. UV/Vis (CH_2Cl_2): $\lambda_{max.}$ (log ε) = 233.0 (4.68), 275.0 (4.38), 284.0 (4.38), 546.0 (3.98) nm. FAB-MS (NBOH): *m*/*z* (%) = 760 (100) [M^+], 611 (34) [$M^+ - O_2CC(O)Ph$]. $C_{38}H_{35}N_4O_5PRu$ (759.76): calcd. C 60.07, H 4.64, N 7.37; found C 60.04, H 4.90, N 7.57.

Complex **8** was also obtained in similar yield and purity either by reaction of the chloro complex **1** with thallium benzoylformate (**4**) or by reaction of benzoylformic acid with **6** or **7**. Crystals of **8** suitable for X-ray structure determination were obtained from a solution of 1,2-dichloroethane with traces of MeOH and H_2O (400:2:1, v/v/v).

[Ru(bdmpza){$O_2CC(O)CH_2CH_2CO_2H$}(PPh_3)] (9): Reaction of [Ru(bdmpza)Cl(PPh_3)$_2$] (**1**) (405 mg, 0.446 mmol), thallium acetate (**2**) (130 mg, 0.493 mmol) and 2-oxoglutaric acid (80.0 mg, 0.548 mmol) in CH_2Cl_2 (20 mL) according to method C yielded product **9** as brownish-red microcrystalline powder after 24 h. Yield 320 mg (95%); m.p. 150−160 °C (dec.). **1. Isomer:** ^1H NMR (CD_2Cl_2, 400 MHz): δ = 1.67 (s, 3 H, C^3-CH_3), 1.82 (s, 3 H, $C^{3'}-CH_3$), 2.05 (ddd, J_{AB} = 21.1, $^3J_{H,H}$ = 5.3, $^3J_{H,H}$ = 5.3 Hz, 1 H, CH_2-CO), 2.26 (ddd, J_{AB} = 17.6, $^3J_{H,H}$ = 5.3, $^3J_{H,H}$ = 5.3 Hz, 1 H, CH_2-COOH), 2.34 (s, 3 H, $C^{5'}-CH_3$), 2.37 (ddd, J_{AB} = 17.6, $^3J_{H,H}$ = 8.8, $^3J_{H,H}$ = 5.4 Hz, 1 H, CH_2-COOH), 2.40 (s, 3 H, C^5-CH_3), 2.95 (ddd, J_{AB} = 21.1, $^3J_{H,H}$ = 8.8, $^3J_{H,H}$ = 5.4 Hz, 1 H, CH_2-CO), 5.72 (s, 1 H, H_{pz}), 5.92 (s, 1 H, $H_{pz'}$), 6.51 (s, 1 H, CH), 7.08 (m, 6 H, *o*-Ph), 7.22 (m, 6 H, *m*-Ph), 7.32 (m, 3 H, *p*-Ph) ppm. ^{13}C NMR (CD_2Cl_2, 100.5 MHz): δ = 11.0 ($C^{5'}-CH_3$), 11.6 (C^5-CH_3), 13.0 ($C^{3'}-CH_3$), 13.9 (C^3-CH_3), 26.9 (CH_2-CO_2H), 34.5 (CH_2-CO), 68.6 (CH), 109.2 (C^4), 109.5 (d, $^4J_{C,P}$ = 2.7 Hz, $C^{4'}$), 128.6 (d, $^3J_{C,P}$ = 9.3 Hz, *m*-PPh_3), 130.1 (d, $^4J_{C,P}$ = 2.5 Hz, *p*-PPh_3,), 131.0 (d, $^1J_{C,P}$ = 40.7 Hz, *i*-PPh_3), 134.1 (d, $^2J_{C,P}$ = 10.1 Hz, *o*-PPh_3), 142.2 ($C^{5'}$), 144.4 (C^5), 155.0 (d, $^3J_{C,P}$ = 2.5 Hz, $C^{3'}$), 159.3 (C^3), 169.2 (CO_2^-), 169.3 (CO_2^-), 174.1 (CO_2H), 215.5 (C=O) ppm. ^{31}P NMR ($CDCl_3$, 161.8 MHz): δ = 58.2.

2. Isomer: ^1H NMR (CD_2Cl_2, 400 MHz): δ = 1.76 (s, 3 H, C^3-CH_3), 1.84 (s, 3 H, $C^{3'}-CH_3$), 2.36 (s, 3 H, $C^{5'}-CH_3$), 2.41 (s, 3 H, C^5-CH_3), 3H covered by the other isomer, 2.83 (ddd, J_{AB} = 21.7, $^3J_{H,H}$ = 8.5, $^3J_{H,H}$ = 6.2 Hz, 1 H, CH_2-CO), 5.74 (s, 1 H, H_{pz}), 5.91 (s, 1 H, $H_{pz'}$), 6.50 (s, 1 H, CH), 7.08 (m, 6 H, *o*-Ph), 7.22 (m, 6 H, *m*-Ph), 7.32 (m, 3 H, *p*-Ph) ppm. ^{13}C NMR (CD_2Cl_2, 100.5 MHz): δ = 11.0 ($C^{5'}-CH_3$), 11.6 (C^5-CH_3), 12.9 ($C^{3'}-CH_3$), 13.8 (C^3-CH_3), 26.8 (CH_2-CO_2H), 34.6 (CH_2-CO), 68.8 (CH), 108.9 (C^4), 109.5 (d, $^4J_{C,P}$ = 2.9 Hz, $C^{4'}$), 128.7 (d, $^3J_{C,P}$ = 12.2 Hz, *m*-PPh_3), 130.0 (*p*-PPh_3), 132.2 (d, $^3J_{C,P}$ = 10.0 Hz, *o*-PPh_3), 141.9 ($C^{5'}$), 143.6 (C^5), 155.2 (d, $^3J_{C,P}$ = 2.6 Hz, $C^{3'}$), 157.9 (C^3), 167.5 (CO_2^-), 168.6 (CO_2^-), 173.6 (CO_2H), 216.8 (C=O) ppm. ^{31}P NMR ($CDCl_3$, 161.8 MHz): δ = 57.1 ppm. IR (CH_2Cl_2): $\tilde{\nu}$ = 1657 vs (CO_2^-), 1563 w (C=N), 1483 w, 1463 w, 1435 m, 1417 w cm^{-1}. IR (KBr): $\tilde{\nu}$ = 1653 vs (CO_2^-), 1560 w (C=N), 1482 w, 1465 w, 1436 w, 1420 w cm^{-1}. UV/Vis (CH_2Cl_2): $\lambda_{max.}$

(log ε) = 235.0 (4.38), 268.0 (3.84), 275.0 (3.85), 294.0 (3.84), 463.0 (3.36) nm. FAB-MS (NBOH): *m/z* (%) = 756 (100) [M^+], 611 (50) [$M^+ - O_2CC(O)CH_2CH_2CO_2H$], 566 (30) [$M^+ - CO_2 - HO_2CC(O)CH_2CH_2CO_2H$]. $C_{35}H_{35}N_4O_7PRu$ (755.73): calcd. C 55.63, H 4.67, N 7.41; found C 55.17, H 4.76, N 7.44.

Complex **9** was also obtained in similar yield and purity either by reaction of the chloro complex **1** with thallium 2-oxoglutarate (**5**) or by reaction of 2-oxoglutaric acid with **6** or **7**.

[Ru(bdmpza){$O_2CC(O)CH_3$}(PPh_3)] (10): Reaction of [Ru(bdmpza)Cl(PPh_3)$_2$] (**1**) (440 mg, 0.484 mmol), thallium acetate (**2**) (157 mg, 0.596 mmol) and pyruvic acid (145 mg, 1.65 mmol) in CH_2Cl_2 (40 mL) according to method C yielded product **10** as brownish-red microcrystalline powder after 2 h. Yield 323 mg (96%); m.p. 250 °C (dec.). ^{1}H NMR ($CDCl_3$, 250 MHz): δ = 1.78 (s, 3 H, C^3 or $C^{3'}-CH_3$), 1.91 (s, 3 H, C^3 or $C^{3'}-CH_3$), 2.07 [s, $C(O)CH_3$], 2.46 (s, 3 H, C^5 or $C^{5'}-CH_3$), 2.47 (s, 3 H, C^5 or $C^{5'}-CH_3$), 5.77 (s, 1 H, H_{pz} or $H_{pz'}$), 5.97 (s, 1 H, H_{pz} or $H_{pz'}$), 6.46 (s, 1 H, CH), 7.19−7.38 (m, 15 H, PPh_3) ppm. ^{13}C NMR ($CDCl_3$, 62.9 MHz): δ = 11.1 (C^5 or $C^{5'}-CH_3$), 11.6 (C^5 or $C^{5'}-CH_3$), 13.3 (C^3 or $C^{3'}-CH_3$), 14.1 (C^3 or $C^{3'}-CH_3$), 25.9 [$C(O)CH_3$], 69.0 (CH), 108.9 (C^4 or $C^{4'}$), 109.2 (C^4 or $C^{4'}$), 128.3 (d, $^3J_{C,P}$ = 9.8 Hz, *m*-PPh_3), 129.7 (*p*-PPh_3), 131.2 (d, $^1J_{C,P}$ = 42.3 Hz, *i*-PPh_3), 134.0 (d, $^2J_{C,P}$ = 8.9 Hz, *o*-PPh_3), 141.1 (C^5 or $C^{5'}$), 143.2 (C^5 or $C^{5'}$), 154.4 (C^3 or $C^{3'}$), 159.1 (C^3 or $C^{3'}$), 168.2 (CO_2^-), 169.3 (CO_2^-), 215.8 (C=O) ppm. ^{31}P NMR ($CDCl_3$, 161.8 MHz): δ = 58.1 ppm. IR (CH_2Cl_2): $\tilde{\nu}$ = 1656 vs (CO_2^-), 1563 w (C=N), 1483 w, 1463 w, 1435 w, 1418 w cm^{-1}. IR (KBr): $\tilde{\nu}$ = 1669 s, 1653 vs (CO_2^-), 1560 w (C=N), 1482 w, 1460 w, 1433 m, 1420 w cm^{-1}. UV/Vis (CH_2Cl_2): $\lambda_{max.}$ (log ε) = 241.0 (4.16), 291.0 (3.79), 463.0 (3.32) nm. FAB-MS (NBOH): *m/z* (%) = 698 (100) [M^+], 611 (48) [$M^+ - O_2CC(O)CH_3$], 566 (30) [$M^+ - CO_2 - HO_2CC(O)CH_3$]. $C_{33}H_{33}N_4O_5PRu$ (697.69): calcd. C 56.81, H 4.77, N 8.03; found C 56.32, H 4.78, N 7.74.

[Ru(bdmpza){$O_2CC(O)CH_2CH_3$}(PPh_3)] (11): Reaction of [Ru(bdmpza)Cl(PPh_3)$_2$] (**1**) (327 mg, 0.360 mmol), thallium acetate (**2**) (108 mg, 0.410 mmol) and 2-oxobutyric acid (47 mg, 0.460 mmol) in CH_2Cl_2 (30 mL) according to method C yielded product **11** as a brownish-red microcrystalline powder after 2 h. Yield 248 mg (97%); m.p. 220 °C (dec.). ^{1}H NMR ($CDCl_3$, 600 MHz): δ = 0.95 (t, $^3J_{H,H}$ = 7.0 Hz, 3 H, CH_2CH_3), 1.80 (s, 3 H, $C^{3'}-CH_3$), 1.89 (s, 3 H, C^3-CH_3), 2.09 (dq, J_{AB} = 21.1, $^3J_{H,H}$ = 7.0 Hz, 1 H, CH_2), 2.46 (s, 3 H, $C^{5'}-CH_3$), 2.46 (s, 3 H, C^5-CH_3), 2.66 (dq, J_{AB} = 21.1, $^3J_{H,H}$ = 7.0 Hz, 1 H, CH_2), 5.75 (s, 1 H, $H_{pz'}$), 5.96 (s, 1 H, H_{pz}), 6.45 (s, 1 H, CH), 7.18−7.40 (m, 15 H, PPh_3) ppm. ^{13}C NMR ($CDCl_3$, 62.9 MHz): δ = 6.9 (CH_2CH_3), 11.1 ($C^{5'}-CH_3$), 11.6 (C^5-CH_3), 13.3 (C^3-CH_3), 14.1 ($C^{3'}-CH_3$), 32.7 (CH_2), 68.9 (CH), 108.9 ($C^{4'}$), 109.3 (C^4), 128.4 (d, $^3J_{C,P}$ = 9.8 Hz, *m*-PPh_3), 129.8 (*p*-PPh_3), 131.1 (d, $^1J_{C,P}$ = 42.3 Hz, *i*-PPh_3), 134.0 (d, $^2J_{C,P}$ = 9.8 Hz, *o*-PPh_3), 141.2 ($C^{5'}$), 143.2 (C^5), 154.4 ($C^{3'}$), 159.1 (C^3), 168.5 (CO_2^-), 169.2 (CO_2^-), 217.9 (C=O) ppm. ^{31}P NMR ($CDCl_3$, 161.8 MHz): δ = 58.5 ppm. IR (CH_2Cl_2): $\tilde{\nu}$ = 1655 vs (CO_2^-), 1563 w (C=N), 1483 w, 1462 w, 1435 w, 1418 w cm^{-1}. IR (KBr): $\tilde{\nu}$ = 1670 s, 1658 vs (CO_2^-), 1560 w (C=N), 1482 w, 1460 w, 1435 m, 1420 w cm^{-1}. UV/Vis (CH_2Cl_2): $\lambda_{max.}$ (log ε) = 241.0 (4.10), 268.0 (3.81), 275.0 (3.82), 297.0 (3.83), 457.0 (3.38) nm. FAB-MS (NBOH): *m/z* (%) = 712 (100) [M^+], 611 (36) [$M^+ - O_2CC(O)CH_2CH_3$], 566 (18) [$M^+ - CO_2 - HO_2CC(O)CH_2CH_3$]. $C_{34}H_{35}N_4O_5PRu$ (711.72): calcd. C 57.38, H 4.96, N 7.87; found C 57.13, H 4.96, N 7.84.

[Ru(bdmpza){$O_2CC(O)Ph$}($NCCH_3$}(PPh_3)] (12): A dark purple suspension of [Ru(bdmpza){$O_2CC(O)Ph$}(PPh_3)] (**8**) (141 mg, 0.186 mmol) in acetonitrile (20 mL) was heated under reflux. Within 2 h the reaction mixture changed into a yellow solution. The solvent was reduced in vacuo and the product was precipitated with Et_2O and filtered off. The product **12** was obtained as a yellow microcrystalline powder. Yield 107 mg (72%); m.p. 85 °C (dec.). ^{1}H NMR (CD_3CN, 250 MHz): δ = 1.62 (s, 3 H, CH_3), 1.97 (s, 3 H, CH_3CN), 2.41 (s, 3 H, CH_3), 2.52 (s, 3 H, CH_3), 2.55 (s, 3 H, CH_3), 6.05 (s, 1 H, $H_{pz'}$ or H_{pz}), 6.24 (s, 1 H, $H_{pz'}$ or H_{pz}), 6.68 (s, 1 H, CH), 7.30−7.60 (m, 18 H, PPh_3 & Ph), 7.91 (m, 2 H, *o*-Ph) ppm. ^{31}P NMR (CD_3CN, 161.8 MHz): δ = 49.7 ppm. IR (KBr): $\tilde{\nu}$ = 2277 w (C≡N), 1669 vs (CO_2^-), 1605 s (CO), 1565 w (C=N), 1484 w, 1465 w, 1436 w, 1419 w cm^{-1}. UV/Vis (CH_2Cl_2): $\lambda_{max.}$ (log ε) = 239.0 (4.49), 341.0 nm (2.96). FAB-MS (NBOH): *m/z* (%) = 802 (3) [MH^+], 760 (31) [$M^+ - CH_3CN$], 652 (81) [$M^+ - O_2CC(O)Ph$], 611 (100) [$M^+ - O_2CC(O)Ph - CH_3CN$]. $C_{40}H_{38}N_5O_5PRu$ (800.82): calcd. C 59.99, H 4.78, N 8.75; CHN analysis not obtained due to loss of CH_3CN.

Calculations: DFT-calculations and full geometry optimisations were carried out by using Jaguar 5.0[24] running on Linux-2.4.18−3smp on three Athlon MP 2400+ dual-processor workstations (Beowulf-cluster) parallelised with MPICH 1.2.4. The crystal structure of the ruthenium(II) benzoylformate complex was used as starting geometry. Complete geometry optimisations were carried out on the implemented BP86/LACVP* basis set (using the 6−31G* basis set and Hay−Wadt effective core potentials on Ru). Extended Hückel MO calculations were performed with the program package Hyperchem[25] running on a single Athlon 1.3 GHz workstation with Windows NT 4.0. The HOMO−LUMO gap energies were calculated using standard parameters as given in the program from the optimised structures of the DFT-calculations. Orbital plots were obtained using Maestro 5.1, the graphical interface of Jaguar.[24]

X-ray Structure Determinations: Single crystals of **6** and **8** were mounted with Paratone-N on a glass fibre. A modified Siemens P4-Diffractometer was used for data collection (graphite monochromator, Mo-K_α radiation, λ = 0.71073 Å, scan rate 4−30°min^{-1} in ω). The structures were solved by using direct methods and refined with full-matrix least-squares against F^2 {Siemens SHELX-97}.[26] A weighting scheme was applied in the last steps of the refinement with $w = 1/[\sigma^2(F_o^2) + (aP)^2 + bP]$ and $P = [2F_c^2 + \max(F_o^2,0)]/3$. Hydrogen atoms were included in their calculated positions and refined in a riding model.

In the asymmetric unit of **6**·H_2O one molecule of dichloromethane was found and refined. The hydrogen atom of the coordinated water molecule bridging to O(4) of the acetato ligand was found. Restraints had to be applied to refine the water hydrogen atoms. About 100 different crystallisation experiments were necessary to obtain crystals of **8**. Finally a mixture of 1,2-dichloroethane with traces of methanol and H_2O (400:2:1, v/v/v) was successful. Using this mixture ten out of ten crystallisation experiments yielded suitable crystals of **8** for X-ray structure determination. **8** crystallised with one molecule of water and methanol each, and half a molecule of 1,2-dichloroethane. Restraints were used in the refinement of the 1,2-dichloroethane. The water molecule forms hydrogen bonds to the methanol and the 2-oxo O(5) atom of other asymmetric units. There is also a hydrogen bond between the methanol and a bdmpza O(1) atom of another asymmetric unit. All details and parameters

Table 3. Structure determination details of compounds **6**·H_2O and **8**

	6·H_2O	**8**
Empirical formula	$C_{32}H_{35}N_4O_5PRu \times CH_2Cl_2$	$C_{38}H_{35}N_4O_5PRu \times {}^1/_2C_2H_4Cl_2 \times H_2O \times H_3COH$
Formula mass	772.61	859.27
Crystal colour/habit	orange block	violet block
Crystal system	triclinic	triclinic
Space group	$P\bar{1}$	$P\bar{1}$
a (Å)	10.877(6)	11.814(10)
b (Å)	12.253(6)	12.659(10)
c (Å)	15.085(7)	14.785(14)
α (°)	92.67(2)	91.95(6)
β (°)	108.52(3)	99.54(6)
γ (°)	113.55(3)	114.35(4)
V (Å^3)	1712.5(15)	1974(3)
θ (°)	2.11−26.00	2.14−27.00
h	−1 to 12	−14 to 14
k	−13 to 13	−16 to 14
l	−18 to 18	−18 to 18
F(000)	792	886
Z	2	2
μ(Mo-K_α) (mm^{-1})	0.707	0.559
Crystal size (mm)	0.25 × 0.2 × 0.1	0.6 × 0.5 × 0.4
$D_{calcd.}$ (gcm^{-3})	1.498	1.446
T (K)	188(2)	188(2)
Reflections collected	7680	9979
Independent reflections	6569	8513
Observed reflections [>2σ(I)]	5298	6977
Parameters	421	505
Weight parameter a	0.0532	0.0571
Weight parameter b	2.8749	1.5342
R_1 (obsd.)	0.0504	0.0431
R_1 (overall)	0.0679	0.0593
wR_2 (obsd.)	0.1159	0.1037
wR_2 (overall)	0.1257	0.1123
Diff. peak/hole (e/Å^3)	1.133/−1.190	0.946/−1.235

of the measurements are summarised in Table 3. The structure pictures were prepared with the program Diamond 2.1e.[27] CCDC-222723 (for **6**·H_2O) and -222724 (for **8**) contain the supplementary crystallographic data for this paper. These data can be obtained free of charge at www.ccdc.cam.ac.uk/conts/retrieving.html or from the Cambridge Crystallographic Data Centre, 12 Union Road, Cambridge CB2 1EZ, UK [Fax: (internat.) +44-1223-336-033; E-mail: deposit@ccdc.cam.ac.uk].

Acknowledgments

Generous financial support by the Fonds der Chemischen Industrie (Liebig-Stipendium granted to N. B.) and the European Commission (Copernicus 2 Program, Contract no° ICA2-CT-2000-10002) is gratefully acknowledged. Special thanks to Prof. Dr. H. Fischer for support and discussion. We are indebted to Mr Galetskiy for recording mass spectra, Ms Friemel for 2D NMR experiments and Mr. Haunz for ^{31}P NMR experiments. We acknowledge a generous gift of ruthenium(III) trichloride hydrate by the Degussa AG.

[1] [1a] E. L. Hegg, L. Que Jr., *Eur. J. Biochem.* **1997**, *250*, 625−629. [1b] S. J. Lange, L. Que Jr., *Curr. Opin. Chem. Biol.* **1998**, *2*, 159−172. [1c] L. Que Jr., *Nat. Struct. Biol.* **2000**, *7*, 182−184. [1d] E. I. Solomon, T. C. Brunold, M. I. Davis, J. N. Kemsley, S.-K. Lee, N. Lehnert, F. Neese, A. J. Skulan, Y.-S. Yang, J. Zhou, *Chem. Rev.* **2000**, *100*, 235−349. [1e] M. J. Ryle, R. P. Hausinger, *Curr. Opin. Chem. Biol.* **2002**, *6*, 193−201.

[2] [2a] P. L. Roach, I. J. Clifton, V. Fülöp, K. Harlos, G. J. Barton, J. Hajdu, I. Andersson, C. J. Schofield, J. E. Baldwin, *Nature* **1995**, *375*, 700−704. [2b] P. L. Roach, I. J. Clifton, C. M. H. Hensgens, N. Shibata, C. J. Schofield, J. Hajdu, J. E. Baldwin, *Nature* **1997**, *387*, 827−830.

[3] [3a] K. Valegård, A. C. Terwisscha van Scheltinga, M. D. Lloyd, T. Hara, S. Ramaswamy, A. Perrakis, A. Thompson, H.-J. Lee, J. E. Baldwin, C. J. Schofield, J. Hajdu, I. Andersson, *Nature* **1998**, *394*, 805−809. [3b] H.-J. Lee, M. D. Lloyd, K. Harlos, I. J. Clifton, J. E. Baldwin, C. J. Schofield, *J. Mol. Biol.* **2001**, *308*, 937−948.

[4] Z. Zhang, J. Ren, D. K. Stammers, J. E. Baldwin, K. Harlos, C. J. Schofield, *Nat. Struct. Biol.* **2000**, *7*, 127−133.

[5] I. J. Clifton, L.-C. Hsueh, J. E. Baldwin, K. Harlos, C. J. Schofield, *Eur. J. Biochem.* **2001**, *268*, 6625−6636.

[6] [6a] J. M. Elkins, M. J. Ryle, I. J. Clifton, J. C. Dunning Hotopp, J. S. Lloyd, N. I. Burzlaff, J. E. Baldwin, R. P. Hausinger, P. L. Roach, *Biochemistry* **2002**, *41*, 5185−5192. [6b] J. R. O'Brien, D. J. Schuller, V. S. Yang, B. D. Dillard, W. N. Lanzilotta, *Biochemistry* **2003**, *42*, 5547−5554.

[7] R. C. Wilmouth, J. J. Turnbull, R. W. D. Welford, I. J. Clifton, A. G. Prescott, C. J. Schofield, *Structure* **2002**, *10*, 93−103.

[8] [8a] N. I. Burzlaff, P. J. Rutledge, I. J. Clifton, C. M. H. Hensgens, M. Pickford, R. M. Adlington, P. L. Roach, J. E. Baldwin, *Nature* **1999**, *401*, 721−724. [8b] J. M. Ogle, I. J. Clifton, P. J. Rutledge, J. M. Elkins, N. I. Burzlaff, R. M. Adlington, P. L. Roach, J. E. Baldwin, *Chem. Biol.* **2001**, *8*, 1231−1237. [8c] J. M. Elkins, P. J. Rutledge, N. I. Burzlaff, I. J. Clifton, R. M. Adlington, P. L. Roach, J. E. Baldwin, *Org. Biomol. Chem.* **2003**, *1*, 1455−1460.

[9] [9a] N. Kitajima, H. Fukui, Y. Moro-oka, Y. Mizutani, T. Kitagawa, *J. Am. Chem. Soc.* **1990**, *112*, 6402−6403. [9b] I. B. Gorell, G. Parkin, *Inorg. Chem.* **1990**, *29*, 2452−2456. [9c] N. Kitajima, N. Tamura, H. Amagai, H. Fukui, Y. Moro-oka, Y. Mizutani, T. Kitagawa, R. Mathur, K. Heerwegh, C. A. Reed, C. R. Randall, L. Que Jr., K. Tatsumi, *J. Am. Chem. Soc.* **1994**, *116*, 9071−9085. [9d] C. R. Randall, L. Shu, Y.-M. Chiou, S. Hagen, M. Ito, N. Kitajima, R. J. Lachicotte, Y. Zang, L. Que Jr., *Inorg. Chem.* **1995**, *34*, 1036−1039. [9e] M. Ito, H. Amagai, H. Fukui, N. Kitajima, Y. Moro-oka, *Bull. Chem. Soc. Jpn.* **1996**, *69*, 1937−1945. [9f] T. Ogihara, S. Hikichi, M. Akita, T. Uchida, T. Kitagawa, Y. Moro-oka, *Inorg. Chim. Acta* **2000**, *297*, 162−170.

[10] [10a] Y. Zang, L. Que Jr., *Inorg. Chem.* **1995**, *34*, 1030−1035. [10b] S. K. Mandal, L. Que Jr., *Inorg. Chem.* **1997**, *36*, 5424−5425. [10c] R. Y. N. Ho, M. P. Mehn, E. L. Hegg, A. Liu, M. J. Ryle, R. P. Hausinger, L. Que Jr., *J. Am. Chem. Soc.* **2001**, *123*, 5022−5029.

[11] [11a] E. H. Ha, R. Y. N. Ho, J. F. Kisiel, J. S. Valentine, *Inorg. Chem.* **1995**, *34*, 2265−2266. [11b] S. Hikichi, T. Ogihara, K. Fujisawa, N. Kitajima, M. Akita, Y. Moro-oka, *Inorg. Chem.* **1997**, *36*, 4539−4547. [11c] E. L. Hegg, R. Y. N. Ho, L. Que Jr., *J. Am. Chem. Soc.* **1999**, *121*, 1972−1973. [11d] M.-P. Mehn, K. Fujisawa, E. L. Hegg, L. Que Jr., *J. Am. Chem. Soc.* **2003**, *125*, 7828−7842.

[12] [12a] Y.-M. Chiou, L. Que Jr., *J. Am. Chem. Soc.* **1992**, *114*, 7567−7568. [12b] Y.-M. Chiou, L. Que Jr., *Inorg. Chem.* **1995**, *34*, 3270−3278. [12c] Y.-M. Chiou, L. Que Jr., *J. Am. Chem. Soc.* **1995**, *117*, 3999−4013.

[13] A. Beck, B. Weibert, N. Burzlaff, *Eur. J. Inorg. Chem.* **2001**, 521−527.

[14] A. Beck, A. Barth, E. Hübner, N. Burzlaff, *Inorg. Chem.* **2003**, *42*, 7182−7188.

[15] [15a] Y. Takahashi, S. Hikichi, M. Akita, Y. Moro-oka, *Chem. Commun.* **1999**, 1491−1492. [15b] M. Akita, Y. Takahashi, S. Hikichi, Y. Moro-oka, *Inorg. Chem.* **2001**, *40*, 169−172. [15c]

M. H. V. Huynh, L. M. Witham, J. M. Lasker, M. Wetzler, B. Mort, D. L. Jameson, P. S. White, K. J. Takeuchi, *J. Am. Chem. Soc.* **2003**, *125*, 308−309.
[16] A. López-Hernández, R. Müller, H. Kopf, N. Burzlaff, *Eur. J. Inorg. Chem.* **2002**, 671−677.
[17] [17a] I. Hegelmann, N. Burzlaff, *Eur. J. Inorg. Chem.* **2003**, 409−411. [17b] L. Peters, N. Burzlaff, *Polyhedron* **2004**, *23*, 245−251.
[18] [18a] M. S. K. Niazi, *Bull. Chem. Soc. Jpn.* **1989**, *62*, 1253−1257. [18b] M. B. Fleury, J. C. Dufresne, *Bull. Soc. Chim. Fr.* **1972**, 844−850. [18c] K. V. Kŭnchev, Y. I. Tur'yan, Kh. A. Dinkov, *Russ. J. Gen. Chem.* **1992**, *62*, 311−315. [18d] K. J. Pedersen, *Acta Chem. Scand.* **1952**, *6*, 243−256. [18e] N. Kawabata, I. Higuchi, J.-I. Yoshida, *Bull. Chem. Soc. Jpn.* **1981**, *54*, 3253−3258.
[19] M. S. Sandford, M. R. Valdez, R. H. Grubbs, *Organometallics* **2001**, *20*, 5455−5463.
[20] V. F. Kuznetsov, G. P. A. Yap, H. Alper, *Organometallics* **2001**, *20*, 1300−1309.
[21] E. G. Pavel, J. Zhou, R. W. Busby, M. Gunsior, C. A. Townsend, E. I. Solomon, *J. Am. Chem. Soc.* **1998**, *120*, 743−753.
[22] R. Hoffman, *J. Chem. Phys.* **1963**, *39*, 1397−1412.
[23] R. Hoffmann, R. Stowasser, *J. Am. Chem. Soc.* **1999**, *121*, 3414−3420.
[24] Jaguar 5.0, Schrödinger, LLC, Portland, Oregon, **2002**.
[25] HyperChem(TM), Hypercube, Inc., 1115 NW 4th Street, Gainesville, Florida 32601, USA.
[26] G. M. Sheldrick, SHELX-97, Programs for Crystal Structure Analysis, University of Göttingen, Göttingen (Germany), **1997**.
[27] K. Brandenburg, M. Berndt, Diamond − Visual Crystal Structure Information System, Crystal Impact GbR, Bonn (Germany), **1999**; for Software Review see: W. T. Pennington, *J. Appl. Crystallogr.* **1999**, *32*, 1028−1029.

Received November 5, 2003
Early View Article
Published Online April 1, 2004

